

8046
✓

The Canadian Journal of Chemical Engineering

Vol. 63

APR. 1985

No. 2



10
E5

The Canadian Journal of Chemical Engineering

CONTENTS

Articles

- Turbulence Model Predictions of the Radial Jet — A Comparison of $k-\epsilon$ Models — P. E. Wood and C. P. Chen 177
- Spray Cone Angle and its Correlation in a High Pressure Fuel Spray — K. S. Varde 183
- An Axisymmetric Model of Flow in the Annulus of a Spouted Bed of Coarse Particles. Model, Experimental Verification and Residence Time Distribution — Howard Littman, Morris H. Morgan, III, Pallassana V. Narayanan, Seung Jai Kim, Jenn-Yuan Day and G. M. Lazarek 188
- Liquid Phase Axial Mixing in a Bubble Column with Viscous Non-Newtonian Liquids — W. D. Devine, Y. T. Shah and B. I. Morsi 195
- Application of the Fourier Transform to the Measurement of $K_L a_L$ in Non-Mechanically Agitated Contactors — G. Andre, M. Moo-Young and C. W. Robinson 202
- A Model for Liquid-Liquid Extraction Column Performance — The Influence of Drop Size Distribution on Extraction Efficiency — S. H. Zhang, S. C. Yu, Y. C. Zhou and Y. F. Su 212
- Pyrolysis of Western Canadian Coals in a Spouted Bed — A. Jarallah and A. P. Watkinson 227
- A Study of the Voltage and Current Efficiencies of Fused Salt, $AlCl_3$ Electrolysis Using Bench Scale Cells — Trausti Hauksson and Frank R. Foulkes 237
- Breakup of Relatively Low-Concentrated O/W Emulsion Jets — Yoshiro Kitamura, Kyoko Kizu and Teruo Takahashi 244
- Peat Adsorption of Herbicide 2,4-D from Wastewaters — Jean-Noel Cloutier, Anh Leduy and Rubens S. Ramalho 250
- Stabilisation of Emulsion Droplets by Fine Powders — S. Levine and E. Sanford 258
- The Catalytic Cracking of a Fischer-Tropsch Synthesis Product — I. Kobilakis and B. W. Wojciechowski 269
- Catalytic Cracking and Skeletal Isomerization of *n*-Hexenes on HY Zeolite — J. Abbot and B. W. Wojciechowski 278
- The Dissolution of Activated Titanium Slag in Dilute Sulfuric Acid — Ivo Toromanoff and Fathi Habashi 288
- Vapour Liquid Equilibrium Calculations for Dilute Aqueous Solutions of CO_2 , H_2S , NH_3 and $NaOH$ to $300^\circ C$ — Bruce E. Roberts and Peter R. Tremaine 294
- Vapor-Liquid Equilibria of the Acetylacetone-1,3-Dioxolane System — Fabio Comelli and Romolo Francesconi 301
- Isobaric Vapor-Liquid Equilibrium in Mixtures of *m*- and *p*-Xylenes with Carbon Tetrachloride — Romolo Francesconi and Fabio Comelli 306
- Computer Simulation of the Fluid and Plasma Protein Transport in the Lungs — Joel L. Bert and Kenneth L. Pinder 309
- Optimization by Lumped Control of Reactors with Langmuir-Hinshelwood Catalyst Deactivation — Juan Ramón González-Velasco, Miguel Angel Gutiérrez-Ortiz and Arturo Romero Salvador 314

Notes to the Editor

- Evaluating Errors in Chemical Plant Mass Balance — C. B. D. Tine 322
- Particle Residence Times in the Continuous Spouting of Mixtures — H. H. Cook and J. Bridgwater 326
- Correlations for Bubble Characteristics in Fluidized Beds — K. Viswanathan 332

A Model for Liquid-Liquid Extraction Column Performance — The Influence of Drop Size Distribution on Extraction Efficiency

S. H. ZHANG, S. C. YU, Y. C. ZHOU and Y. F. SU

East-China Institute of Chemical Technology, Shanghai 201107, China

A precise model for predicting liquid-liquid extraction column efficiency based upon assumed hydrodynamic, axial mixing and mass transfer behaviour has been formulated and solved numerically.

The complex nature of the dispersed phase can be better described by drop-size-dependent residence time distribution (RTD). Both the variation of axial velocities due to drops of different sizes, i.e. forward mixing, and the axial dispersion for the drops of the same size have been considered in this model.

The computed results reveal that the effects of both varying velocities and dispersion of drops on extraction efficiency are appreciable and cannot be neglected, and the efficiency may be overestimated if only a forward mixing model is adopted. The comparison of the experimental values of N_{ODP} with those predicted shows that the mass transfer data obtained in RDC agree well with the values predicted by the present model for the case of solute transfer in $c \rightarrow d$ direction, and are slightly higher than the predicted ones for the transfer in $d \rightarrow c$ direction.

On a formulé et résolu numériquement un modèle précis pour prévoir l'efficacité d'une colonne d'extraction liquide-liquide basé sur un comportement hydrodynamique hypothétique, le mélange axial et le transfert de masse ayant été formulés et résolus numériquement.

On peut mieux décrire la nature complexe de la phase dispersée par une distribution de temps de séjour qui dépend de la dimension des gouttes. On a considéré, dans ce modèle, à la fois la variation des vitesses axiales avec la dimension des gouttes (mélange avancé) et la dispersion axiale pour les gouttes de mêmes dimensions.

Les résultats calculés révèlent que l'effet de la variation des vitesses et celui de la dispersion des gouttes sur l'efficacité d'extraction sont appréciables et ne peuvent être négligés; l'efficacité peut être surestimée si seul un modèle de mélange avancé est adopté. La comparaison des valeurs expérimentales de N_{ODP} avec les valeurs prédites indique que les données de transfert de matière obtenues dans RDC concordent bien avec les valeurs prévues par ce modèle dans le cas du transfert du soluté dans la direction $c \rightarrow d$; les valeurs expérimentales sont légèrement plus élevées que les valeurs prévues dans le cas du transfert dans la direction $d \rightarrow c$.

The problem of axial mixing in liquid-liquid extraction columns has been studied intensively in the past twenty or more years. The influence of axial mixing in one or both phases was included, but each phase was assumed to be a continuum either in a dispersion model or in a back-flow model.

Studies on axial mixing in the continuous phase in RDC or pulsation columns show that it may be successfully described by a dispersion model. In applying the dispersion model to the dispersed phase, it is assumed that the concentration of the dispersed phase keeps constant throughout a given cross-section of the column due to sufficiently intensive coalescence and redispersion. This assumption is not always satisfied in normal operating conditions especially when there is a low holdup and relatively mild agitation. In such cases the probability of the collision of drops is not large, rather, the coalescence of drops is hindered by impurities. Consequently, a constant concentration of drops throughout the column cross-section might not be established.

In fact, the dispersed phase in extraction columns covers a wide range of drop size distribution. The large drops pass through the column more rapidly than the drops of average size do (the forward mixing effect). The small ones reside for a longer time and may even be highly backmixed owing to their lower inertia. Accordingly, different drops may have their own different concentrations and mass transfer coefficients even if they are at the same cross-section of the column.

Olney (1964) was the first one who accounted for the

discontinuous character of the dispersed phase and the distribution of drop diameters. It was assumed that each drop size fraction in the dispersion contributes to the overall column performance in terms of its own residence time and mass transfer rate. Similarly, Rod (1966) analysed the effect of the varying velocities of drops of different sizes (forward mixing) with the back-mixing and suggested an approximate method for calculating column height.

However, the effect of residence time distribution of drops on both the mass transfer behaviour and the concentration driving force of the drops was not taken into account.

Recently, Chartres and Korchinsky (1975) solved the forward-mixing model numerically. The solution included the estimation of the dispersed phase mass transfer coefficients from single drop models and the continuous phase coefficients. Experimental evidence of the influence of drop size was obtained by Korchinsky and Cruz-Pinto (1979, 1980).

Using stochastic process theory, this paper presents a model in which the RTD related to the drop diameter is introduced so that not only the forward and back-mixing but also the mass transfer behaviour of drops are taken into account.

Theoretical modelling

THE STATISTICAL STUDY ON DROP MOVEMENT

The flow pattern of two phases usually is countercurrent in an extraction column. One of the two phases is dispersed

C^*	= liquid phase equilibrium concentration (kmol/m ³)
C_s	= concentration of cellulose fibers (kg/m ³)
d_B	= mean bubble diameter (m)
E	= electrical signal from IR analyzer (V)
$F(s), F(j\omega)$	= transfer function and its Fourier transform
$G(s), H(s)$	= intermediate transfer functions
Im	= imaginary part of a complex number
j	= $(-1)^{0.5}$
k_L	= liquid film mass transfer coefficient (m/s)
$K_L a_L$	= overall volumetric gas-liquid mass transfer coefficient based on the gas-free volume of liquid or of slurry (s ⁻¹)
n	= index of frequency
n_{max}	= number of frequencies
n_o	= number of orifices in the sparger
P	= number of well-mixed stages in the gas phase
Q_G	= volumetric flowrate of the gas stream (at 101.33 kPa and 25°C) (m ³ /s)
Re	= real part of a complex number
s	= Laplace domain variable (s ⁻¹)
St_G	= Stanton number for the gas phase (Equation (4))
T	= period of the Fourier series (s)
t	= time (s)
u_{SG}	= superficial gas velocity (m/s)
V_G	= volume of the gas phase held up in the contactor (m ³)
V_L	= volume of gas-free liquid or slurry (m ³)
$Y(t), Y_i(t)$	= dimensionless responses of the IR analyzer to a step input, to an impulse

Greek letters

α	= calibration factor of the IR analyzer [$\bar{E}(t = \infty) / \bar{C}_G(t = \infty)$]
ϵ	= fractional gas hold-up
λ	= dimensionless solubility of CO ₂ [$= \bar{C}_L(t = \infty) / \bar{C}_G(t = \infty)$]
τ_D	= pure time delay in response curves (s)
τ_G	= "hydraulic" residence time in the gas phase (s)
τ_M	= time constant of the gas sampling and collecting train (s)
Φ	= objective function (Equation (5))
ω, ω_n	= angular frequency in the definition of the Fourier transform

Subscripts

exp	= experimental value
FB	= finite level of backmixing in the gas phase
i	= stage number
l	= impulse
L	= liquid
mod	= model
PF	= plug-flow in the gas phase
WM	= well-mixed gas phase

Superscripts

-	= deviation variable (with respect to initial steady state)
\hat{Y}	= Fourier transform of $Y(t)$

References

- Akita, K., F. Yoshida, "Bubble Size, Interfacial Area and Liquid-Phase Mass Transfer Coefficient in Bubble Columns", *Ind. Eng. Chem. Process Des. Dev.* **13**, 84 (1974).
- André, G., M. Moo-Young and C. W. Robinson, "Improved Method for the Dynamic Measurement of Mass Transfer Coefficient for Application to Solid Substrate Fermentation", *Bio-*

- technol. Bioeng.* **23**, 1611 (1981).
- André, G., "Mixing and Mass Transfer Studies of a Novel Gas-Liquid-Solid Contactor for Application to Solid Substrate Fermentations", Doctoral Dissertation, University of Waterloo, Waterloo, Ontario (1982).
- André, G., C. W. Robinson and M. Moo-Young, "New Criteria for Application of the Well-Mixed Model to Gas-Liquid Mass Transfer Studies", *Chem. Eng. Sci.* **38**, 1845 (1983).
- Bhavaraju, S. M., T. W. F. Russell and H. W. Blanch, "The Design of Gas Sparged Devices for Viscous Liquid Systems", *A.I.Ch.E. J.* **24**, 454 (1978).
- Beveridge, G. S. G. and R. S. Schechter, "Optimization: Theory and Practice", McGraw-Hill, New York, pp. 180-189 (1970).
- Calderbank, P. H., "Mass Transfer in Fermentation Equipment", in *Biochemical and Biological Engineering Science*, N. Blakebrough, Edr., Academic Press, London (1967).
- Calderbank, P. H., M. B. Moo-Young, "The Continuous Phase Heat and Mass-Transfer Properties of Dispersions", *Chem. Eng. Sci.* **16**, 39 (1961).
- Calderbank, P. H., D. S. L. Johnson and J. Loudon, "Mechanics and Mass Transfer of Single Bubble in Free Rise", *Chem. Eng. Sci.* **25**, 235 (1970).
- Chandrasekharan, K. and P. H. Calderbank, "The evaluation of mass transfer product from unsteady-state gas absorption/desorption", *Chem. Eng. Sci.* **35**, 1473 (1980).
- Deckwer, W.-D., Personal communication (1981).
- Dunn, I. J. and A. Einsele, "Oxygen transfer coefficients by the dynamic method", *J. Appl. Chem. Biotechnol.* **25**, 707 (1975).
- Figueiredo, M. M. L. and P. H. Calderbank, "The Scale-up of Aerated Mixing Vessels for Specified Oxygen Dissolution Rates", *Chem. Eng. Sci.* **34**, 1333 (1979).
- Gangwal, S. K., "Reliability and Limitations of Pulsed Chromatography as a Method of Obtaining Properties of Flow Systems", Doctoral Thesis, University of Waterloo, Waterloo, Ontario (1975).
- Gangwal, S. K., R. R. Hudgins and P. L. Silvestro, "Reliability and Limitations of Pulse Chromatography as a Method of Obtaining Properties of Flow Systems", *Can. J. Chem. Eng.* **57**, 609 (1979).
- Himmelblau, D. M., "Process Analysis by Statistical Methods", John Wiley & Sons, New York (1970).
- Levenspiel, O., "Chemical Reaction Engineering", 2nd Edition, John Wiley & Sons, New York (1972).
- Mangartz, K. H. and T. Pilhofer, "Untersuchungen zur Gasphasendispersion in Blasensäulen Reaktoren", *Vorfahrtstechnik*, **14**, 40 (1980).
- Moo-Young, M. and H. W. Blanch, "Design of Biochemical Reactors: Mass Transfer Criteria for Simple and Complex Systems", in *Advances in Biochemical Engineering*, A. Fiechter, Edr., Springer-Verlag, Berlin (1981), **19**, pp. 1-69.
- Mukataka, S., H. Kataoka and J. Takabashi, "Effect of Vessel Size and Rheological Properties of Suspensions on the Distribution of Circulation Times in Stirred-Vessels", *J. Ferment. Technol.* **58**, 155 (1980).
- Ramachandran, P. A. and J. M. Smith, "Transport Rates by Moment Analysis of Dynamic Data", *Ind. Eng. Chem. Fundam.* **17**, 148 (1978).
- Schumpe, A. and W.-D. Deckwer, "Estimation of O₂ and CO₂ Solubilities in Fermentation Media", *Biotechnol. Bioeng.* **21**, 1075 (1979).
- Spiegel, M. R., "Advanced Calculus", McGraw-Hill, New York, pp. 299 (1963).
- Wernau, W. C., "Mass Transfer to Newtonian and non-Newtonian Systems in Stirred-Tank Contactors", Doctoral dissertation, Univ. of California, Berkeley (1972).

Manuscript received March 19, 1984; revised manuscript received October 11, 1984; accepted for publication October 18, 1984.

into drops due to the agitation or pulsation. As long as there is a sufficient intensity of agitation in the column, the concentration of the continuous phase at a given cross-section may be regarded as constant. So the continuous phase is a microflow, but the dispersed phase is not. When the holdup is low and the agitation is not very vigorous, the probability of collision among drops is small. A uniform concentration of the drop phase throughout a given cross-section of the column cannot be well developed. Each drop still retains its own identity. Hence it is a macroflow.

Many types of agitated or pulsed extraction column usually consist of a series of compartments, in and between which the drops move stochastically under agitation or pulsation. The residence times of the drops are diversified and the moving paths of the drops are also different from each other, even if they are of the same diameter. Besides, the dispersion does have a drop size distribution (DSD) and the motions of the drops are related to their diameters. Therefore, neither the concentration of the individual drops, which have passed the column section and gathered at the interface, nor the concentration of the drops at any given cross-section of the column is the same. There exists a concentration distribution of dispersed phase at any cross-section.

To consider the law of drop movement, the following assumptions have been made:

- i) drops of different diameters possess different average axial velocities which are related to the terminal velocities of the drops;
- ii) only drops of equal size possess the same axial dispersion coefficient;
- iii) moving conditions of drops of equal size are equivalent, and the random movements of the drops in the column can be approached by using stochastic process theory.

With the help of the previous two assumptions, the complex moving nature of the drops concerning drop size distribution can be simplified into the superimposed stochastic results of several fractions of equal-size drops. According to probability theory, if the conditional transition probability of the individual drop is achieved, the movements of the swarms of drops can be predicted.

THE MOVING LAW OF EQUAL-SIZE DROPS — THE MARKOV PROCESS, CONTINUOUS IN SPACE AND TIME

In view of a swarm of equal-size drops the position of the individual drop, $Z(\tau)$, is a stochastic process with a parameter of time τ . If time is fixed, Z is a stochastic variable.

The following assumptions can be made through the observation of drop movement:

- i) the process of movement is not affected by the previous history of the drop;
- ii) the track of the moving drop is continuous;
- iii) the drop has a finite average velocity at any time;
- iv) in a very small interval of time, $\Delta\tau$, the average square deviation of the displacement of the drop is proportional to the time interval, $\Delta\tau$, but homogeneous to the time.

Such a stochastic process can be regarded as a time-homogeneous Markov process in which time and states are continuous. It is also called a diffusion process.

The Fokker-Planck equation is a special type of Kolmogorov equation describing this situation. The alternative name of Fokker-Planck equation is the "Forward Second Kolmogorov Equation" or the "Generalized Diffusion Equation".

Equation (1) is a one-dimensional Fokker-Planck Equation

$$\frac{\partial f(t, w; \tau, Z)}{\partial \tau} = - \frac{\partial}{\partial Z} [a(\tau, Z)f(t, w; \tau, Z)] + \frac{1}{2} \frac{\partial^2}{\partial Z^2} [b(\tau, Z)f(t, w; \tau, Z)] \quad (1)$$

where $f(t, w; \tau, Z)$ = the transition probability density; t, τ = time ($\tau > t$); and w, Z = the position of the drop at time t and τ respectively.

Let $a(\tau, Z) = U$, the average velocity of the drop, and $b(\tau, Z)/2 = E_D$, the axial dispersion coefficient of the drop, then Equation (1) becomes

$$\frac{\partial f(t, w; \tau, Z)}{\partial \tau} = - U \frac{\partial}{\partial Z} f(t, w; \tau, Z) + E_D \frac{\partial^2}{\partial Z^2} f(t, w; \tau, Z) \quad (2)$$

It is a parabolic partial differential equation with two independent variables. Using Laplace transformation, one of the variables, such as time variable τ , can be removed. The partial differential equation then reduces to an ordinary differential equation which can be solved. Subsequently, the transform is converted back to a function of the two independent variables which gives the transition probability density of the diffusion equation.

Let $f^*(s, Z)$ be the Laplace transform of $f(t, w; \tau, Z)$

$$f^*(s, Z) = \mathcal{L}\{f(t, w; \tau, Z)\} = \int_0^\infty f(t, w; \tau, Z) \exp(-s\tau) d\tau \quad (3)$$

Equation (2) can be transformed into

$$sf^* - f(0^+) = E_D \frac{d^2 f^*}{dZ^2} - U \frac{df^*}{dZ} \quad (4)$$

which satisfies the initial condition

$$f(0, Z) = 0 \quad (5)$$

and the boundary condition

$$f(\tau, \infty) = 0 \quad (6)$$

Hence the transform of Equation (2) is

$$E_D \frac{d^2 f^*}{dZ^2} - U \frac{df^*}{dZ} - sf^* = 0 \quad (7)$$

Equation (7) is a second order linear ordinary differential equation. The eigenequation of Equation (7) is

$$E_D m^2 - Um - s = 0 \quad (8)$$

where

$$m_1 = \frac{U + \sqrt{U^2 + 4E_D s}}{2E_D}$$

and

$$m_2 = \frac{U - \sqrt{U^2 + 4E_D s}}{2E_D} \quad (9)$$

m_1 and m_2 are eigenvalues. It is obvious that $m_1 > 0$ and $m_2 < 0$. Then the two linearly independent solutions are as follows:

$$f_1^*(s, Z) = \exp(m_1 Z) \\ f_2^*(s, Z) = \exp(m_2 Z) \quad (10)$$

The solutions should satisfy the boundary condition. As Z approaches infinity, both f and f^* should remain finite. Therefore, we have

$$f^*(s, Z) = f_2^*(s, Z) = \exp \left[\left(\frac{U - \sqrt{U^2 + 4E_D s}}{2E_D} \right) Z \right] \dots \dots \dots (11)$$

Inverting Equation (11) by using Laplace transform gives

$$f(t, w; \tau, Z) = \frac{U}{\sqrt{4\pi E_D(\tau - t)}} \times \exp \left\{ -\frac{[Z - w - U(\tau - t)]^2}{4E_D(\tau - t)} \right\} \dots \dots \dots (12)$$

$f(t, w, \tau, Z)$ is the transition probability density submitted to the Fokker-Planck (Equation (2)). From Equation (12), the age distribution of drops at the exit can be written as

$$f(0, 0; \tau, L) = \frac{U}{\sqrt{4\pi E_D \tau}} \exp \left\{ -\frac{(L - U\tau)^2}{4E_D \tau} \right\} \dots \dots (13)$$

and the age distribution of drops at the cross-section of height Z is

$$f(0, 0; \tau, Z) = \frac{U}{\sqrt{4\pi E_D \tau}} \exp \left\{ -\frac{(Z - U\tau)^2}{4E_D \tau} \right\} \dots \dots (14)$$

THE EFFECT OF DSD ON RTD

Equation (14) is, in fact, the conditional transition probability density related to the drop size. Hence it can be rewritten as

$$f(\tau, Z | d) = f_i(0, 0; \tau, Z) \dots \dots \dots (15)$$

If the drop size shows no effect on the transition probability density, i.e. no segregation,

$$f(\tau, Z) = f(\tau, Z | d) \dots \dots \dots (16)$$

which can be used to predict the RTD of all kinds of drops regardless of the drop sizes.

The drops usually, however, have DSD and segregation effects. Therefore, using the statistical method, the overall RTD of drops at the cross-section of height Z is given by

$$E(\tau, Z) = \frac{\int_0^\infty v(d)U(d)f(\tau, Z | d)dd}{\int_0^\infty \int_0^\infty v(d)U(d)f(\tau, Z | d)ddd\tau} \dots \dots (17)$$

and the overall age distribution of drops at the exit is

$$E(\tau, L) = \frac{\int_0^\infty v(d)U(d)f(\tau, L | d)dd}{\int_0^\infty \int_0^\infty v(d)U(d)f(\tau, L | d)ddd\tau} \dots \dots (18)$$

where $v(d)$ is the volumetric distribution density of the drop with diameter d in dispersed phase, and $U(d)$ is the vertical (axial) velocity of the drop with diameter d .

The axial dispersion coefficient of drop E_D in Equations (12)–(14) is an important parameter. Olney (1964) assumed that E_D was a constant which could apply to all the drops of all sizes in a given operation circumstance. Later Rod (1968) proved experimentally that the assumption was not valid. After measuring the residence time of sieved individual solid particles, he evaluated the diffusional component

of the dispersed phase in RDC and recommended a correlation as below

$$\frac{E_D}{UH\tau} = 0.7 + 0.02 \frac{ND_R \epsilon}{U} \dots \dots \dots (19)$$

where ϵ is the fractional free cross-section.

The correlation (19) implies that E_D is dependent on the geometry of the column, the rotating speed and the vertical velocity of the drop and is independent directly of its own physical properties. If E_D , $v(d)$, $U(d)$ are known, the overall age distribution of drops can be predicted by Equations (14, 17, 18).

STATISTICAL STUDY ON EXTRACTION COLUMN PERFORMANCE

1. The case of constant concentration in the continuous phase

If the concentration of continuous phase does not change appreciably, it can be regarded as a constant concentration which is the average value at inlet and outlet. It is approximately true when

- the throughput of the continuous phase is much greater than that of the dispersed phase; and
- the height of the column is low, the number of compartments is small, and back-mixing is very serious.

Then the mass transfer coefficient and the concentration of drop are dependent on its RTD only. Combining Equation (20) with Equation (14) to calculate RTD, the concentration of dispersed phase at outlet and the extraction efficiency of the column can be evaluated.

The mass transfer equation for a single drop is

$$\frac{dy_i}{d\tau} = -\frac{6}{d_i} K_{OD_i}(\tau)(y_i - y^*) \dots \dots \dots (20)$$

Since $x = \text{constant}$, therefore $y^* = F(x) = \text{constant}$. Integrating Equation (20), the concentration of the drop can be obtained

$$y_i - y^* = (y_0 - y^*) \exp \left\{ -\frac{6}{d_i} \int_0^\tau K_{OD_i}(\tau) d\tau \right\} \dots (21)$$

The overall concentration of dispersed phase at outlet is equal to the mean of the concentrations of the drops approaching the interface.

$$Y = \frac{\int_{d_{\min}}^{d_{\max}} \int_0^\infty y(\tau, d) f(\tau, L | d) \varphi(d) d\tau dd}{\int_{d_{\min}}^{d_{\max}} \varphi_i \int_0^\infty y_i(\tau) f_i(\tau, L) d\tau dd} \dots \dots \dots (22)$$

2. The case of continuous phase with a concentration profile

If there is a concentration profile in the continuous phase, the extraction efficiency of a drop depends not only on its RTD, but also on what path it has travelled. Since the movement of the drop is random, where and how long the drop has resided are stochastic. It obeys a Markov process. Hence y^* in Equation (20) is a stochastic variable. It should be pointed out that the concentration of drop y_i in Equation (20) is affected by its earlier history. So it is difficult to solve the problem mathematically without certain simplifications.

To consider the performance model, the following assumptions are noted:

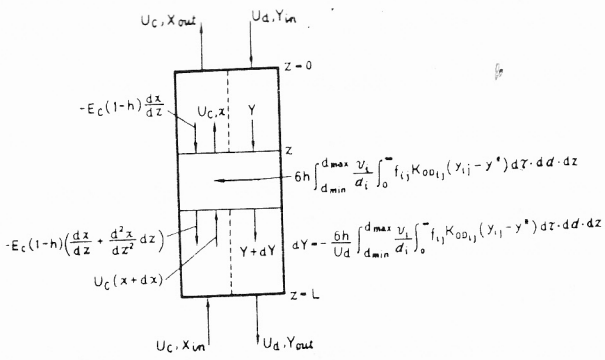


Figure 1 — Performance model of extraction column.

- i) coalescence and redispersion rarely occur due to the low holdup,
- ii) concentrations of the solute in both phases are low, hence the flow rates of the two phases can be regarded as steady,
- iii) the drops are spherical,
- iv) there is no extra interfacial resistance. The overall mass transfer coefficient can be evaluated by using a two-resistance model,
- v) the mass transfer coefficients of the drop-side phase can be predicted by using models derived for a single drop, such as the rigid drop model (Newman model), the laminar circulating model (Kronig-Brink model), or the turbulent circulating model (Handlos-Baron model) respectively, according to the Reynolds number of the drops,
- vi) the drop at certain time and position has covered its prior path at an average moving speed. It has been proved that the probability corresponding to this assumption is maximum. Hence the assumption is acceptable.

According to the assumption vi), the concentration of the drop can be calculated by Equation (23):

$$\frac{dy(\tau, d)}{d\tau} = -\frac{6K_{OD}(\tau, d)}{d} [y(\tau, d) - y^*] \dots \dots \dots (23)$$

Making the material balance of the height element dZ (see Figure 1) a set of integral-differential equations has been derived.

For the drops of diameter d ,

$$\frac{dy(d)}{dZ} = -\frac{6}{dU(d)} \int_0^\infty K_{OD}(\tau, d) [y(\tau, d) - y^*] \times f(\tau, Z|d) d\tau \dots \dots \dots (24)$$

The overall concentration of the dispersed phase is

$$Y = \int_{d_{min}}^{d_{max}} \varphi(d)y(d)dd \dots \dots \dots (25)$$

where $\varphi(d)$ is the density of the flowrate of the drop-size. It can be defined as

$$\varphi(d) = U(d)v(d) / \int_{d_{min}}^{d_{max}} U(d)v(d)dd \dots \dots \dots (26)$$

Differentiating Equation (25) and combining with Equation (24), Equation (27) can be derived.

$$\frac{dY}{dZ} = -\frac{6h}{U_d} \int_{d_{min}}^{d_{max}} \int_0^\infty K_{OD}(\tau, d) [y(\tau, d) - y^*] \times f(\tau, Z|d) \frac{v(d)}{d} d\tau dd \dots \dots \dots (27)$$

Since it is difficult to solve the model equations analytically, a sophisticated numerical computer programme has been developed.

The spectrum of drop-size distribution has been divided into several fractions, e.g. n fractions. In addition, the duration of residence time has been divided into several intervals, e.g. m intervals. Thus the Equations (23) and (27) can be reduced to

$$\frac{dy_{ij}}{dZ} = -\frac{6K_{OD_{ij}}(y_{ij} - y^*)}{d_i U_{ij}} \dots \dots \dots (28)$$

where $i = 1, 2, 3, \dots, n$ respect to n drop-size fractions, and $j = 1, 2, 3, \dots, m$ respect to m time intervals.

$$\frac{dY}{dZ} = -\frac{6h}{U_d} \int_{d_{min}}^{d_{max}} \frac{v_i}{d_i} \int_0^\infty f_{ij} K_{OD_{ij}} (y_{ij} - y^*) d\tau dd \dots \dots (29)$$

The total solute transferred per unit area within the differential height, dZ , equals to

$$6h \int_{d_{min}}^{d_{max}} \frac{v_i}{d_i} \int_0^\infty f_{ij} K_{OD_{ij}} (y_{ij} - y^*) d\tau dd dZ \dots \dots \dots (30)$$

For the continuous phase, the material balance gives

$$E_c \frac{d^2x}{dZ^2} + \frac{U_c}{(1-h)} \frac{dx}{dZ} + \frac{6h}{(1-h)} \int_{d_{min}}^{d_{max}} \frac{v_i}{d_i} \int_0^\infty f_{ij} K_{OD_{ij}} \times (y_{ij} - y^*) d\tau dd = 0 \dots \dots \dots (31)$$

X is a hypothetical concentration which represents the concentration of continuous phase of plug-flow. Equation (31) can be reduced to Equation (32) and (33).

$$\frac{dX}{dZ} = -\frac{6h}{U_c} \int_{d_{min}}^{d_{max}} \frac{v_i}{d_i} \int_0^\infty f_{ij} K_{OD_{ij}} (y_{ij} - y^*) d\tau dd \dots \dots (32)$$

$$E_c \frac{dx}{dZ} = \frac{U_c}{(1-h)} (X - x) \dots \dots \dots (33)$$

where f_{ij} is the age distribution of the drops, it can be evaluated by Equation (14), $v(d)$ is the volumetric density of the drops and v_i is the volumetric fraction of the drops.

The boundary conditions are:

$$\begin{aligned} Z = 0, \quad Y = Y_{in} \\ \frac{dx}{dZ} = 0, \quad \text{therefore } x = x_{out} \dots \dots (34) \\ Z = L, \quad x = x_{in} - \frac{E_c(1-h)}{U_c} \left(\frac{dx}{dZ} \right)_{Z=L} \\ Y = Y_{out} \end{aligned}$$

Thus, the model consisting of a set of integral-differential equations, including Equations (28), (29), (32), (33) and boundary conditions (34), usually has hundreds of differential equations. A computer-programmed solution has been developed.

After from the above theoretical performance model, the calculation or measurement of the following parameters is required in column design or performance prediction:

- i) drop size distribution;
- ii) drop velocity distribution and dispersed phase holdup;
- iii) mass transfer coefficients of both drop side and continuous phase;
- iv) axial dispersion coefficients of continuous phase.

DROP SIZE DISTRIBUTION (DSD)

Drop size distribution depends strongly on the type and speed of the agitator, the direction of mass transfer, flow-rates and physical properties of the system. For the time being, it cannot be predicted precisely. It has to be measured experimentally to obtain accurate predictions of column performance.

In the present study, a photographic technique was used to measure the drop sizes and size distributions during each run. The Mugele-Evans distribution function (Equation (35)) was used to fit the experimental data of drop size distribution.

$$v(d) = \frac{\delta}{\sqrt{\pi}} \frac{d_{\max}}{d(d_{\max} - d)} \exp \left\{ - \left[\delta \ln \left(\frac{ad}{d_{\max} - d} \right) \right]^2 \right\} \quad (35)$$

This is the upper limit log-normal distribution. Olney (1964), Chartres and Korchinsky (1975) and Jeffreys et al. (1981) had confirmed that the drop size distribution in RDC is better described by the Mugele-Evans distribution.

It is usually adopted that the logarithm of the drop size is plotted against the cumulative percentage less than that size on a probability scale in order to calculate the parameters of the distribution. Such a method is rather tedious. Instead of this graphical method, a parameter-fitting method was used. The parameters in the Mugele-Evans distribution function were evaluated from the measurement in each run in order to obtain the least-squares error between function-calculated and experimental data. The procedure of computation is as follows.

Define the observed volumetric distribution of the drops less than size $(d_i + r_i/2)$ as $V_{i,\text{obsv}}$

$$V_{i,\text{obsv}} \left(d_i + \frac{r_i}{2} \right) = \frac{\sum_{d_{\min}}^{d_i} n_i d_i^3}{\sum_{d_{\min}}^{d_{\max}} n_i d_i^3} \quad (36)$$

where r_i is the width of the interval of drop diameter. Using Mugele-Evans distribution, the calculated volumetric distribution of the drops less than size $(d_i + r_i/2)$ is

$$V_{i,\text{calc}} \left(d_i + \frac{r_i}{2} \right) = \int_{d_{\min}}^{d_i+r_i/2} \frac{\delta}{\sqrt{\pi}} \frac{d_{\max}}{d(d_{\max} - d)} \exp \left\{ - \left[\delta \ln \left(\frac{ad}{d_{\max} - d} \right) \right]^2 \right\} dd \quad (37)$$

Define the deviation of observations as Ψ_i

$$\Psi_i(\mathbf{x}) = V_{i,\text{obsv}} - V_{i,\text{calc}}(\mathbf{x}) \quad (38)$$

where \mathbf{x} is the vector of the parameters

$$\mathbf{x} = (x_1, x_2, \dots, x_m) \quad (39)$$

let

$$x_1 = a, \text{ asymmetrical distribution parameter} \quad (40)$$

$$x_2 = \delta, \text{ uniformity distribution parameter}$$

The d_{\max} in Equation (37) is a parameter which may take the value of the maximum drop diameter in the picture. Usually only one drop is maximum. If there are N values of the observed drop-size data, the vector of the function is

$$\Psi(\mathbf{x}) = [\Psi_1(\mathbf{x}), \Psi_2(\mathbf{x}), \dots, \Psi_N(\mathbf{x})]^T \quad (41)$$

Let the objective function be $\|\Psi(\mathbf{x})\|^2$, and search the optimum parameters to make the objective function have its minimum value, i.e.

$$\|\Psi(\mathbf{x})\|^2 = \Psi(\mathbf{x})^T \Psi(\mathbf{x}) \rightarrow \text{minimum} \quad (42)$$

It is a non-linear optimisation problem. A damped least square method was used.

DROP VELOCITY DISTRIBUTION

To approach the problem of drop velocity distribution, it is better to measure the values of drop velocities, which will undoubtedly be highly dependent on drop size. But such measurements have not been made so that the approximate method proposed by Olney (1964) and Chartres and Korchinsky (1975) was adopted here.

The assumption is that the drop velocity relative to the continuous phase is proportional to the terminal velocity of the single drop. Misek and Marek (1970) proposed a correlation of the drop terminal velocity in RDC.

$$U_i = 0.249d \left(\frac{g^2 \Delta \rho}{\rho_c \mu_c} \right)^{1/3} \quad (43)$$

Olney (1964) and Chartres and Korchinsky (1975) suggested that the drop velocity distribution is found by combining Equations (44, 45).

$$U_i = U_{s,i} - U_c / (1 - h) = C' C_R U_{t,i} (1 - h) - \frac{U_c}{(1 - h)} \quad (44)$$

where C_R is Olney's constriction factor and

$$C' = \left[\frac{U_d}{h} + \frac{U_c}{(1 - h)} \right] / \int_{d_{\min}}^{d_{\max}} C_R v_i U_{t,i} (1 - h) dd$$

and

$$\frac{U_d}{h} = \int_{d_{\min}}^{d_{\max}} v_i U_i dd \quad (45)$$

where h is the dispersed phase holdup which was measured experimentally in each run.

MASS TRANSFER COEFFICIENTS

The measurement of drop size dependent mass transfer coefficient in an operating extraction column would require techniques not yet demonstrated. For the time being, it seems more logical to assume a model for a single drop to predict drop-side and continuous phase mass transfer coefficients, and to compare them with the data taken from the single drop experiments.

When a drop is small, it behaves like a rigid sphere. Newman (1931) solved the diffusion equation of a rigid sphere model. The instantaneous coefficient for a rigid sphere is given by

$$k_{d,s} = \frac{2\pi^2 D_d \sum_{n=1}^{\infty} \exp\left[-\frac{4n^2\pi^2 D_d \tau}{d^2}\right]}{3d \sum_{n=1}^{\infty} \frac{1}{n^2} \exp\left[-\frac{4n^2 D_d \tau}{d^2}\right]} \dots\dots\dots (46)$$

Similarly, Kronig-Brink (1950) using Hadamard streamline equation derived a laminar circulating model. The instantaneous mass transfer coefficient for the model is obtained as follows:

$$k_{d,L} = \frac{32D_d \sum_{n=1}^{\infty} A_n^2 \lambda_n \exp\left[-\lambda_n \frac{64D_d \tau}{d^2}\right]}{3d \sum_{n=1}^{\infty} A_n^2 \exp\left[-\lambda_n \frac{64D_d \tau}{d^2}\right]} \dots\dots\dots (47)$$

In large drops, oscillation as well as internal circulation has been observed. The motion within the drop was assumed by Handlos and Baron (1957) to be highly turbulent, who derived a model which took account of the vibrations of the drop as well as the circulation. The experimental studies showed that the model was generally applied to oscillating drops.

$$k_{d,T} = \frac{U_s}{768(1 + \mu_d/\mu_c)} \times \frac{\sum_{n=1}^{\infty} \lambda_n B_n^2 \exp\left[-\frac{\lambda_n U_s \tau}{128(1 + \mu_d/\mu_c)}\right]}{\sum_{n=1}^{\infty} B_n^2 \exp\left[-\frac{\lambda_n U_s \tau}{128(1 + \mu_d/\mu_c)}\right]} \dots\dots\dots (48)$$

Take the first eigenvalue, $\lambda_1 = 2.88$, the approximate coefficient is given by

$$k_{d,T} = \frac{0.00375 U_s}{1 + \mu_d/\mu_c} \dots\dots\dots (49)$$

Strictly speaking, the three models given above are based upon the assumption that no mass transfer resistance exists in the continuous phase. In the present study, the main resistance to mass transfer resides in the dispersed phase since the equilibrium distribution of the solute favors the aqueous phase. Hence, only minor errors would be introduced by using the equations given above.

Although there are three drop mass transfer models available, how to choose the particular one remains unsolved. An attempt was made in this paper to find the criterion based on earlier experimental studies. Johnson (1960) and Zhang et al. (1963) published vast amounts of mass transfer data of single drop experiments. They revealed that the mass transfer data of the drop-side matched the Kronig-Brink model only when the Reynolds number of the drop was less than 50. Beyond 50, the value of the mass transfer coefficient for the drop-side would increase rapidly with the Reynolds number, but it could reach only 30%–70% of that predicted value suggested by Handlos-Baron model.

To extend the scope of using drop mass transfer models, it has been suggested that the criterion for choosing the models is the drop Reynolds number ($Re = dU_s \rho_c / \mu_c$), i.e.:

$Re \leq 1.0$, the rigid sphere model (Newman) is used;

$50 \geq Re > 1.0$, the laminar circulating model (Kronig-Brink) is used;

TABLE 1
Geometric Factors of RDC

D_T , cm	D_s , cm	D_R , cm	H_T , cm	Number of compartments
10.0	6.75	5.0	2.50	40

$Re > 50$, 50% predicted value of Handlos-Baron model is adopted

$$\dots\dots\dots (50)$$

To evaluate the mass transfer coefficients of the continuous phase, the Calderbank and Moo-Young correlation (1961) for agitated vessels was used. The overall mass transfer coefficient was then obtained from the individual coefficients, k_d and k_c , by

$$\frac{1}{K_{OD}} = \frac{1}{k_d} + \frac{m}{k_c} \dots\dots\dots (51)$$

AXIAL DISPERSION COEFFICIENTS OF CONTINUOUS PHASE

A considerable amount of work has been done in this aspect and empirical correlations are available for several types of columns. In the present study, the following correlation, suggested by Zhang et al. (1981), was used to predict the dispersion coefficient for the agitated zone of the column.

$$\frac{E_c}{U_c H_T} = 0.5 + 0.0204 \left(\frac{D_s}{D_T}\right)^{1.75} \left(\frac{D_T}{H_T}\right)^{0.5} \left(\frac{D_R N}{U_c}\right)^{0.74} \times \left(\frac{U_d + U_c}{U_c}\right)^{0.52} \dots\dots\dots (52)$$

This relationship is analogous to those proposed by Miyauchi et al. (1966). However, the effect of the dispersed phase flow rate on the dispersion coefficient of the continuous phase has been included. For the settling zone the correlation of Vermeulen et al. (1966) was used.

Experimental

APPARATUS

A rotating disk contactor, diameter 0.1 m, effective height 1.2 m, was used in this study. The effective agitating zone, height 1.0 m, consisted of forty compartments. In the centers of all compartments were situated forty rotating disks of 1 mm thickness which were supported by a common shaft of 16 mm diameter and driven by a D.C. motor. The speed of rotation was measured by an electronic meter. All the internals were made of stainless steel. Above the agitated zone, there was a settling zone of 0.2 m height. The important column parameters are listed in Table 1.

The flow rates of both phases were measured by rotameters. The continuous phase outlet was fitted with a regulating valve and a solenoid valve which could automatically control the main interface at the top end of the column. The heavy and light phases were supplied to the column from two head tanks. A schematic flowsheet is shown in Figure 2.

The equipment for measuring RTD of the dispersed phase is illustrated in Figure 3. A sample collector, 40 mm diameter, was fitted in the settling zone just under the inter-

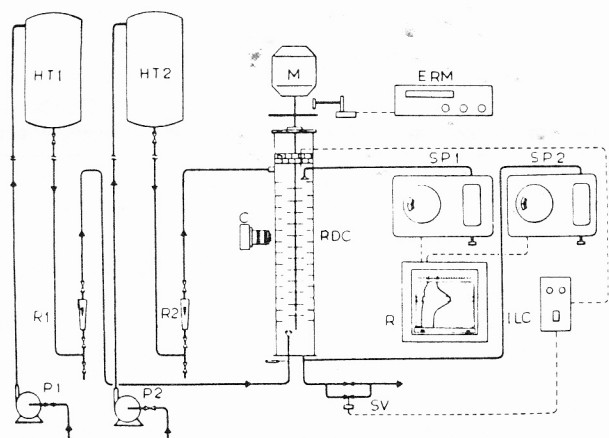


Figure 2 — Schematic flowsheet of experimental equipment: C, camera; ERM, electronic rotation speed meter; HT1,2, head tank; ILC, interfacial level controller; M, D.C. motor; P1,2, pump; R, recorder; R1,2, rotameter; SP1,2, spectrophotometer; SV, solenoid valve.

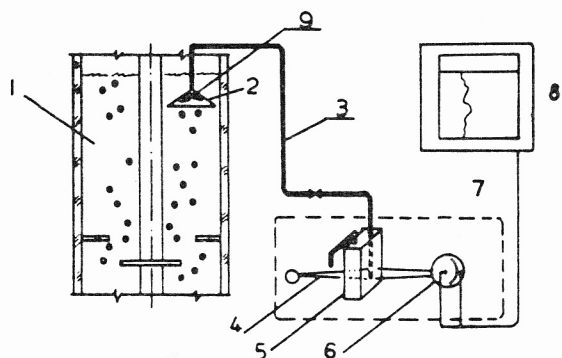


Figure 3 — Schematic configuration of apparatus for measuring RTD of dispersed phase: 1, RDC; 2, sample collector; 3, 2 mm dia. Teflon tube; 4, light beam; 5, quartz cell; 6, photo cell; 7, spectrophotometer; 8, recorder; 9, wire mesh.

face. In the sample collector there was a piece of wire mesh which just allowed the organic phase to pass through. The sampled organic phase then flowed through a Teflon tube of 2 mm diameter into a quartz cell which was put in the spectrophotometer.

SYSTEM

Water-kerosene-*n*-butyric acid system was used with water as the continuous phase, kerosene as the dispersed phase and butyric acid as the transferring solute. Organic chemicals of technical grade were used.

In axial mixing experiments, the pulse injection technique was used. Two red dyes have been chosen. One was acid red only soluble in aqueous phase, and the other, candle red, was only soluble in organic phase. No interference between phases was observed in the axial mixing experiments.

The physical properties of the system were measured experimentally as shown in Table 2.

In mass transfer runs, the values of the physical properties of both inlet and outlet streams were measured and the

TABLE 2
Typical Physical Properties

System (no solute)	Viscosity c.p.	Density g/cm ³	Interfacial tension dyne/cm
Method	Ostwald viscometer	Westphal balance	Drop weight
Water	1.01	1.000	42.0
Kerosene	2.51	0.806	

arithmetic mean values were taken for mass transfer calculations.

Before the mass transfer runs were carried out, two phases were mutually saturated by the extraction column in order to ensure conditions of essentially single component mass transfer. The solute concentration of the raffinate at the inlet was kept at low levels, about 30 g/L and the solute concentration in incoming solvent was nearly 0 g/L.

PROCEDURE

To start the operation, the experimental RDC was first filled with the continuous phase, then the dispersed phase was gradually introduced. The motor was started and set at a proper speed. In each run, after a certain volume of continuous phase corresponding to more than five times the total volume of the column has passed through the column, and the samples were analysed several times, to ensure that steady state had been established. At the end of each run all inlet and outlet samples were collected and analysed, then the run was stopped for holdup measurement. Only the data for which the solute mass balance checked within 5% were accepted. All dispersed phase holdups were determined by the displacement method, i.e. shutting-off all the valves on the inlet and outlet streams at the same time, then allowing the phases to separate before measuring the dispersed phase volume. The concentration of solute in the samples was measured by titration.

The procedure for determination of axial mixing effect was to inject a pulse of tracer (1 mL dye solution) and to sample downstream or at the outlet. Samples were analysed with a spectrophotometer (characteristic wavelength of 540 nm). The response curves were recorded. The sample flowrate was regulated and measured, and the volume of the Teflon tube and cell etc., were fixed, so the delay of the response curve could be evaluated.

Absorbance is the logarithm of the ratio between the intensities of the light beam before entering and after leaving the sample, i.e. the logarithm of reciprocal transmittance.

$$C \propto A$$

$$A = \log \left(\frac{1}{T} \right) = 2 - \log (100T) \dots \dots \dots (53)$$

The drop size in the RDC were determined photographically using a camera equipped with an extension tube located at the middle of the column. A diffused flash light source was used for illumination. From the enlarged photographs over one hundred drops were measured in each photo to evaluate the drop size distribution.

Solute distribution data were measured experimentally

TABLE 3
Parameters of Drop Size Distribution (no Mass Transfer)

Exp. no.	U_c cm/s	U_d cm/s	N 1/s	d_{32} cm	d_{max} cm	a	δ	h
101	0.246	0.0724	9.17	0.228	0.366	0.287	0.481	0.0516
102	0.286	0.0724	9.17	0.296	0.438	0.246	0.618	0.0586
103	0.338	0.0724	9.17	0.290	0.420	0.237	0.512	0.0597
104	0.386	0.0724	9.17	0.235	0.402	0.430	0.460	0.0465
105	0.481	0.0724	9.17	0.265	0.438	0.319	0.418	0.0470
106	0.246	0.0724	10.8	0.202	0.329	0.372	0.635	0.0669
107	0.286	0.0724	10.8	0.252	0.384	0.241	0.443	0.0521
108	0.338	0.0724	10.8	0.257	0.420	0.312	0.545	0.0525
109	0.386	0.0724	10.8	0.254	0.384	0.242	0.549	0.0556
110	0.246	0.0724	11.7	0.168	0.276	0.414	0.544	0.0599
111	0.290	0.0724	11.7	0.166	0.293	0.525	0.567	0.0604
112	0.338	0.0724	11.7	0.186	0.293	0.366	0.709	0.0567
113	0.386	0.0724	11.7	0.174	0.293	0.410	0.582	0.0600
114	0.481	0.0724	11.7	0.164	0.276	0.492	0.664	0.0582
115	0.246	0.0724	13.3	0.130	0.202	0.414	0.804	0.0830
116	0.290	0.0724	13.3	0.139	0.238	0.437	0.815	0.0743
117	0.338	0.0724	13.3	0.106	0.166	0.472	0.808	0.0696
118	0.386	0.0724	13.3	0.115	0.184	0.464	0.771	0.0743
119	0.481	0.0724	13.3	0.111	0.184	0.549	0.783	0.0908
120	0.290	0.0724	15.0	0.109	0.184	0.566	0.785	0.113
121	0.290	0.108	15.0	0.0937	0.166	0.711	1.032	0.191
122	0.386	0.0724	15.0	0.106	0.202	0.769	0.678	0.130

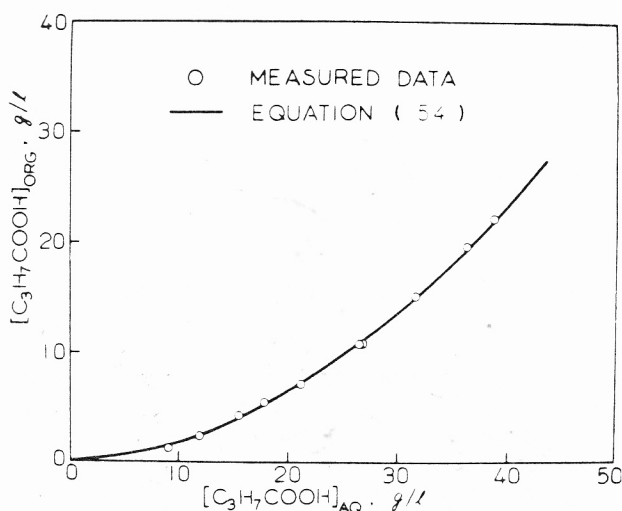


Figure 4 — Measured solute distribution data.

and correlated as below by least squared polynomial regression analysis.

$$y^* = 0.05155x + 0.01320x^2 \dots \dots \dots (54)$$

It is shown together with the data in Figure 4.

Results

DROP SIZE AND DROP SIZE DISTRIBUTION

The experimental condition and Mugele-Evans parameters d_{max} , a and δ determined by damped least square method to fit the experimental data are listed in Table 3. The

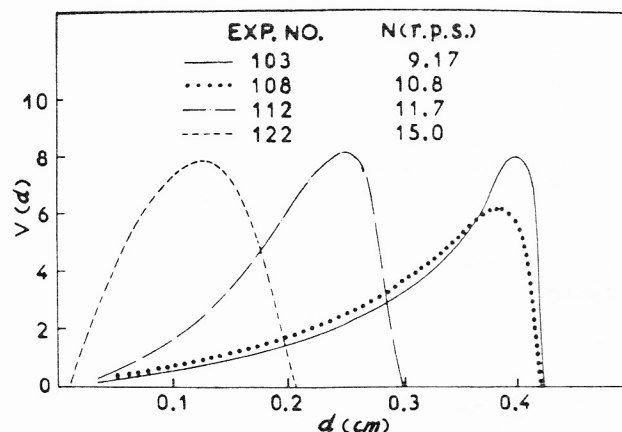


Figure 5 — Comparison of DSD.

Mugele-Evans function with a choice of three parameters promises a more accurate representation, particularly of the large drops, than other functions.

In order to illustrate and compare different DSD in different rotating speed, four DSD curves were drawn in the same figure. The flowrates of both continuous and dispersed phase in these runs were all the same. As Figure 5 shows, the maximum drop size decreases with increasing rotor speed. But the asymmetrical distribution parameters and the uniformity distribution parameters a and δ , increase with increasing rotor speed. That means the higher the rotor speed is, the smaller the drop sizes are, the less asymmetrical and the more uniform the distribution will be.

These upper limit log-normal distributions are in good agreement with the experimental drop size data. The agreement is confirmed by comparing d_{32} calculated from experimental data by Equation (55)

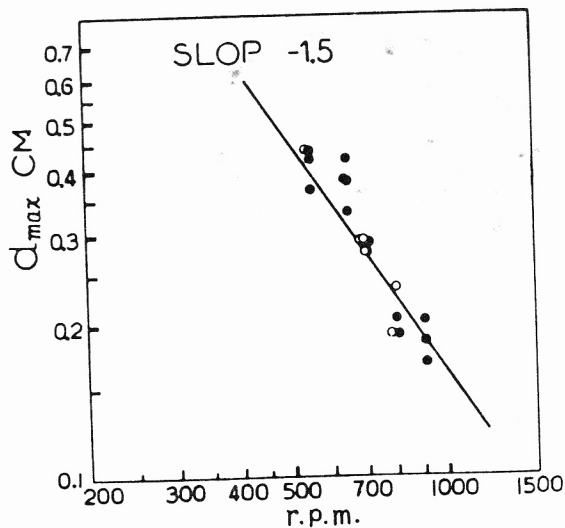


Figure 6 — Rotor speed and d_{max} .

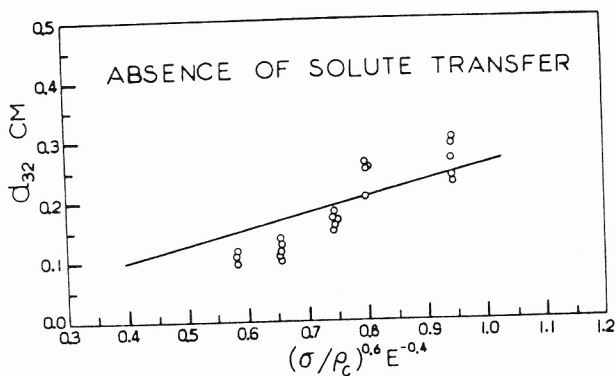


Figure 7 — Correlation of Sauter mean diameters (no solute transfer).

$$d_{32} = \frac{\sum n_i d_i^3}{\sum n_i d_i^2} \dots \dots \dots (55)$$

with d_{32} from the upper limit distribution which is calculated from Equation (56).

$$d_{32} = 1 / \int_0^\infty \frac{v(d)}{d} dd \dots \dots \dots (56)$$

To correlate the maximum drop data or the Sauter mean drop size data, the theory of isotropic turbulence proposed by Hinze (1955) was applied

$$d_{max} = C_1 \left(\frac{\sigma}{\rho_c} \right)^{0.6} E^{-0.4} \dots \dots \dots (57)$$

where E is the rate of energy dissipation per unit mass of fluid. Strand et al. (1962) reported the constant C_1 to be in the range of 0.4 to 0.6, according to the different systems. The maximum drop size data of no solute transfer runs are plotted in Figure 6. The slope of d_{max} vs. rotor speed is -1.5 which is in accordance with Strand's data. However, according to Equation (57), the slope should be -1.2 . The constant C_1 in this study is about 0.45.

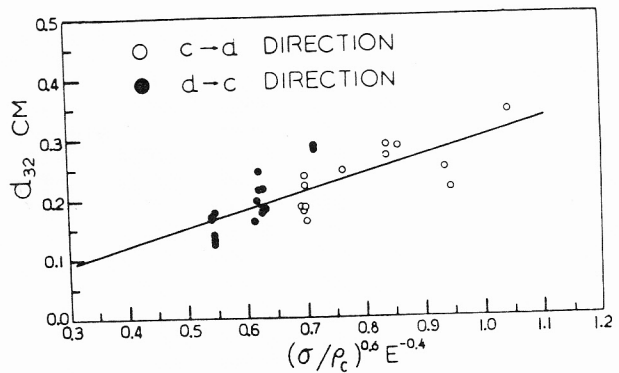


Figure 8 — Correlation of Sauter mean diameters (mass transfer run).

TABLE 4
The Ratio of d_{32} to d_{max}

Mass transfer runs		No mass transfer runs	
Rotor speed r.p.s.	d_{32}/d_{max}	Rotor speed r.p.s.	d_{32}/d_{max}
6.67	0.62	9.17	0.63
8.33	0.69	10.8	0.64
9.17	0.65	11.7	0.60
10.8	0.63	13.3	0.61
12.5	0.59	15.0	0.56

It was suggested that, as a first approximation, the ratio, the Sauter mean diameter/maximum drop diameter, might be taken as a constant. Therefore

$$d_{32} = C_2 \left(\frac{\sigma}{\rho_c} \right)^{0.6} E^{-0.4} \dots \dots \dots (58)$$

In no solute transfer runs, C_2 is approximately equal to 0.27, although the exponent of E also shows a little deviation from -0.4 .

The Sauter mean drop size data were plotted in Figures 7, 8. The data in mass transfer runs are more scattered because they are sensitively affected by solute concentration and the direction of solute transfer.

According to the experimental data, the constants in the correlations of drop size d_{32} in RDC have been obtained.

For mass transfer runs, $C_2 = 0.30$

For no mass transfer runs, $C_2 = 0.27$

The average ratios of d_{32} to d_{max} are listed in Table 4. The data show that as the rotor speed increases, the ratio decreases slightly. On the whole, the average ratio is 0.62.

RESIDENCE TIME DISTRIBUTION OF DISPERSED PHASE

From the transmittance curves on the recording paper, the absorbance data were evaluated by Equation (53). As the concentration of the dye tracer was proportional to the absorbance, the experimental overall age distributions could be calculated by Equation (59).

$$E_{exp}(\tau) = \frac{C(\tau)}{\int_0^\infty C(\tau) d\tau} \dots \dots \dots (59)$$

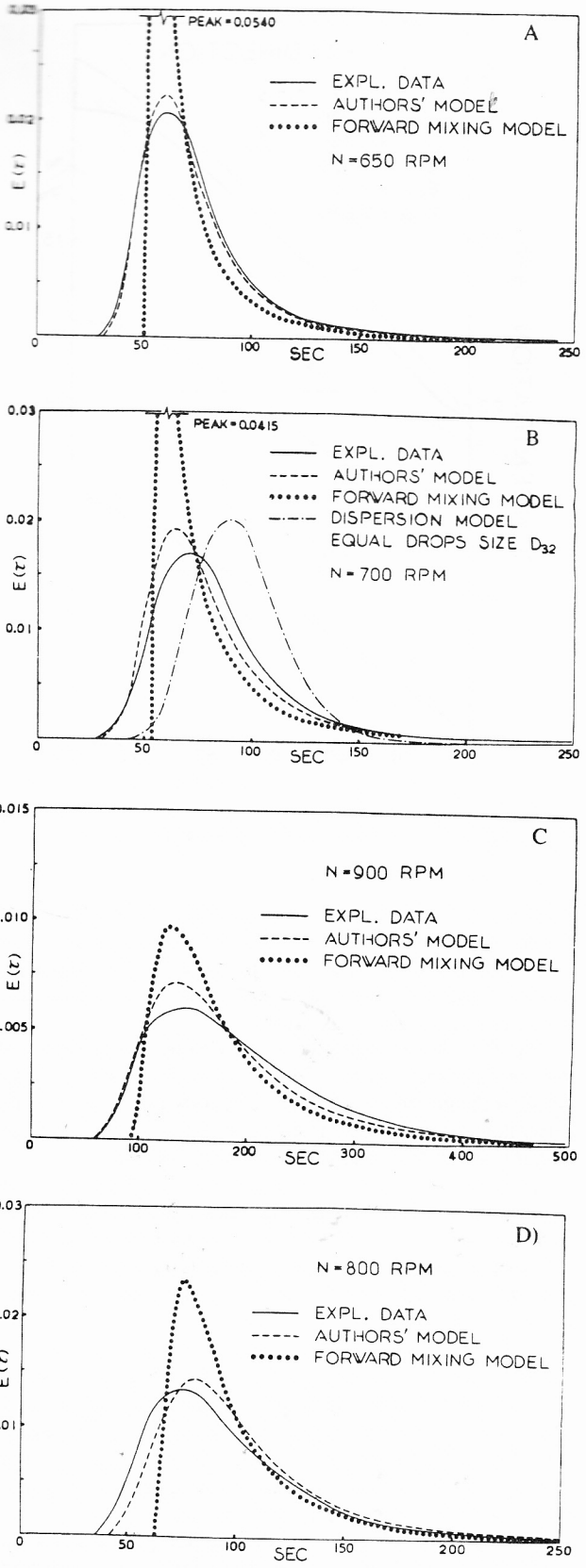


Figure 9 — (A, B, C, D) Overall age distribution of dispersed phase.

The overall age distributions predicted by the model, Equation (18), were computed. Figure 9 gives several examples, in which the distribution curves predicted by the forward mixing model were plotted too.

TABLE 5
Numerical Characteristics of RTD

Exp. no.	μ_1		σ		
	Mean (sec)		Standard deviation (dimensionless)		
Exp.	Exp.	Pred.	Exp.	Pred. by authors' model	Pred. by dispersion model with d_{32}
101	77.9	76.7	0.553	0.527	0.195
102	88.5	91.3	0.729	0.434	0.198
103	90.1	86.4	0.765	0.482	0.199
104	70.2	67.0	0.478	0.626	0.193
105	70.9	65.7	0.478	0.605	0.193
106	101	102	0.651	0.476	0.208
107	78.7	79.1	0.587	0.519	0.199
108	79.2	78.2	0.505	0.519	0.200
109	83.9	86.3	0.534	0.475	0.202
110	90.5	87.9	0.478	0.539	0.207
111	91.2	88.9	0.729	0.570	0.207
112	85.6	87.9	0.609	0.471	0.205
113	90.6	88.5	0.652	0.538	0.207
114	87.9	86.2	0.491	0.553	0.206
115	125	128	0.565	0.433	0.225
116	112	115	0.548	0.451	0.220
117	105	108	0.532	0.475	0.217
118	112	113	0.580	0.482	0.220
119	137	131	0.528	0.503	0.229
120	171	164	0.596	0.451	0.249
121	193	186	0.417	0.429	0.258
122	195	158	0.624	0.494	0.259

The comparison of experimental and model-predicted overall age distributions of dispersed phase (see Figure 9) shows that values predicted by the model, Equations (13, 18), were nearly the same as the experimental values when Misesk axial mixing coefficient, and Olney and Korchinsky approximate method were utilized.

The curves predicted by the forward mixing model usually have much higher peaks than those obtained experimentally, especially when the rotor speed was not very high. Besides, the overall age distribution predicted by the dispersion model based on equal drop-size d_{32} gives less asymmetrical values, i.e. smaller variance and skewness than experimental ones. Hence the greater deviations between experimental overall age distributions and the predicted values by both forward mixing model and dispersion model have been confirmed.

In order to compare more data, the numerical characteristics of distribution were utilized. Table 5 gives the means and standard deviations of the distributions; Figures 10 and 11 give the skewnesses and peak-factors separately.

The following numerical characteristics of distribution were used.

μ_1 = mean, the first moment

$$\mu_1 = \int_0^{\infty} \tau E(\tau) d\tau \dots \dots \dots (60)$$

σ_i^2 = variance

$$\sigma_i^2 = \int_0^{\infty} (\tau - \mu_1)^2 E(\tau) d\tau \dots \dots \dots (61)$$

σ = standard deviation (dimensionless)

$$\sigma = \sqrt{\frac{\sigma_i^2}{\mu_1^2}} \dots \dots \dots (62)$$

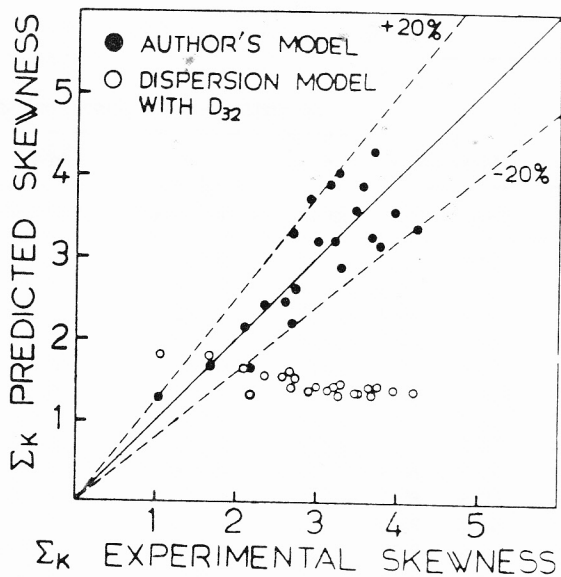


Figure 10 — Predicted vs. experimental skewness.

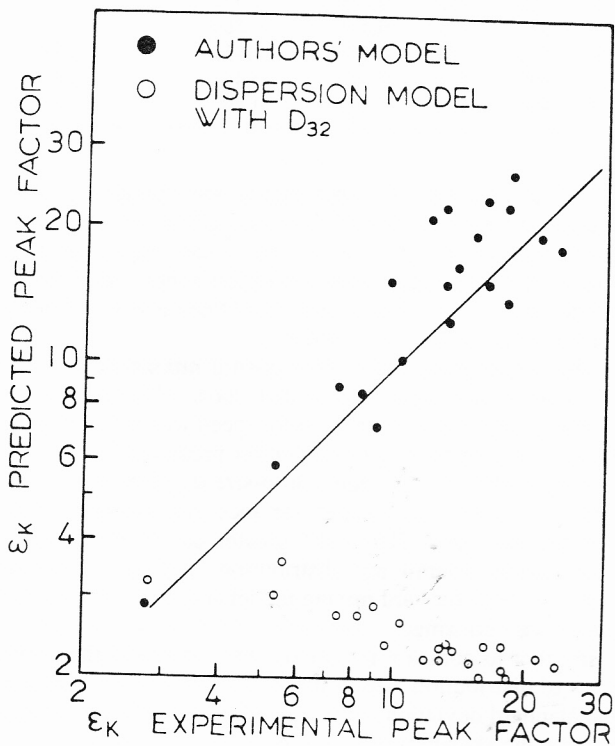


Figure 11 — Predicted vs. experimental peak factor.

Σ_k = skewness

$$\Sigma_k = \frac{\int_0^\infty (\tau - \mu_1)^3 E(\tau) d\tau}{\sigma_t^3} \dots \dots \dots (63)$$

ϵ_k = peak factor

$$\epsilon_k = \frac{\int_0^\infty (\tau - \mu_1)^4 E(\tau) d\tau}{\sigma_t^4} - 3 \dots \dots \dots (64)$$

From Table 5 and Figures 10, 11, good agreement has

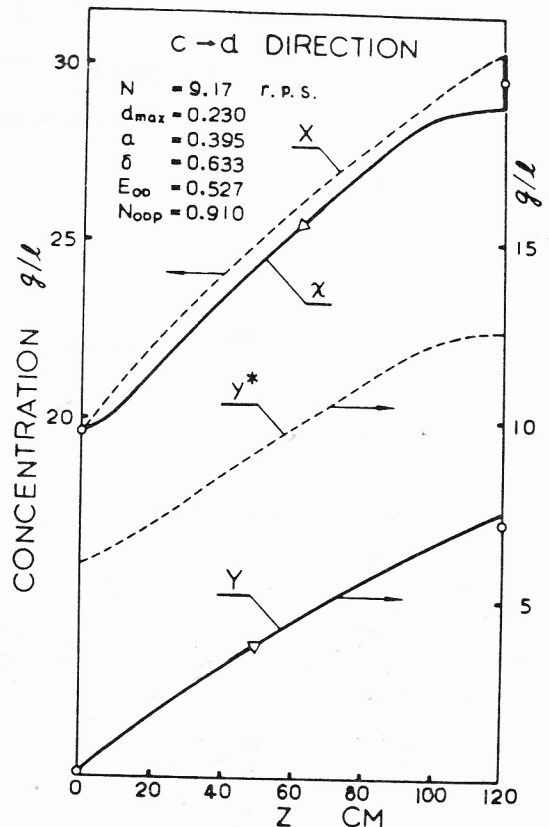


Figure 12 — Concentration profiles predicted for run 7.

been reached between the experimental data and those predicted by the model. Almost all skewness data lie within 20% error lines, whereas those predicted by the dispersion model (equal drop size) show much smaller standard deviation, skewness and peak factor.

The skewnesses predicted by this model agree well with the experimental ones. These skewnesses are positive, which indicate the great influence of forward mixing and the importance of segregation in the swarms of the drops, especially when the agitation is not very intense.

As revealed in Tables 3, 5 and Figure 10, the runs at low agitation speed have greater skewness, peak factor and almost the same standard deviation. It means that the high value of axial mixing at low or mild agitation condition is contributed mainly by different axial velocities of the drops, i.e. forward mixing effect.

As the agitation becomes more vigorous, the drop size becomes smaller and the spectrum of DSD gets narrower. The vertical velocities of drops decrease, whereas the axial dispersion coefficients increase. Consequently, the skewness and peak factor get smaller. In such case, the contribution of dispersion effect to the axial mixing becomes more important than in the previous case.

Although the values of age distribution predicted by our model agree well with the experimental ones, a certain deviation still remains. It seems likely that the errors are mainly introduced by the drop size measurement and the possible existence of coalescence of drops in the column.

MASS TRANSFER OPERATION

To predict the mass transfer efficiencies, the solutions of the single drop model equations leading to the calculation of

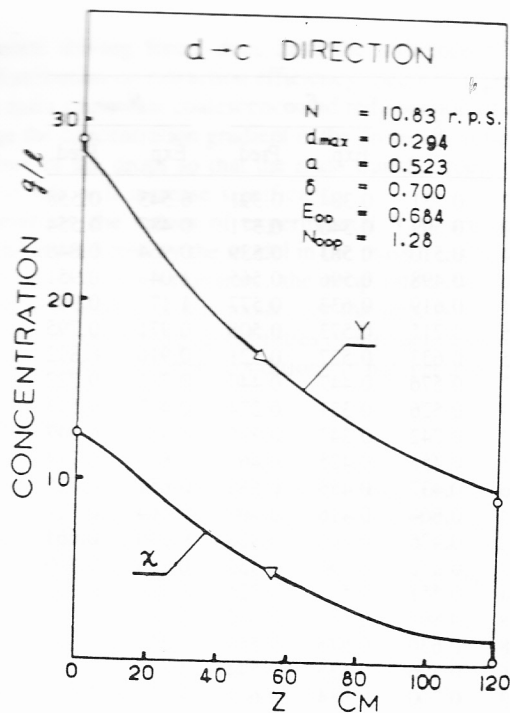


Figure 13 — Concentration profiles predicted for run 20.

overall mass transfer coefficients were substituted directly into Equations (28, 29, 32, 33). These equations with boundary conditions, Equation (34), were then solved to obtain the dispersed and continuous phase concentration profiles, from which the extraction efficiencies and plug-flow number of transfer units were calculated.

Considering that greater deviations were predicted by using only one drop model for mass transfer calculation, a criterion to choose the models was adopted.

Two typical examples of concentration profiles are illustrated in Figures 12 and 13. Dispersed phase-based extraction efficiencies, η_{OD} , and plug-flow number of transfer units, N_{ODP} , were calculated from the concentrations of column inlet and outlet streams by means of Equations (65) and (66).

$$\eta_{OD} = \frac{Y_{out} - Y_{in}}{Y^*(x_{in}) - Y_{in}} \dots \dots \dots (65)$$

$$N_{ODP} = \frac{1}{\lambda - 1} \ln \frac{1 - \eta_{OD}}{1 - \eta_{OD}/\lambda} \dots \dots \dots (66)$$

where $\lambda = U_c / (U_d \cdot m)$.

Mass transfer results are better examined in terms of the plug-flow number of transfer units (based on the dispersed phase concentration) because it is very sensitive.

Extraction efficiencies, predicted by different performance models, are illustrated in Figure 14, in which only Kronig-Brink drop model is used. The difference of the curves is large, confirming the inability of d_{32} to adequately represent the dispersion of drops having varying sizes. If the column height is fixed the plug-flow model gives the highest extraction efficiency, while our model gives the most conservative prediction.

The influence of the performance model chosen for mass transfer calculation increases significantly as the extraction efficiency increases. Predicted heights for achieving a de-

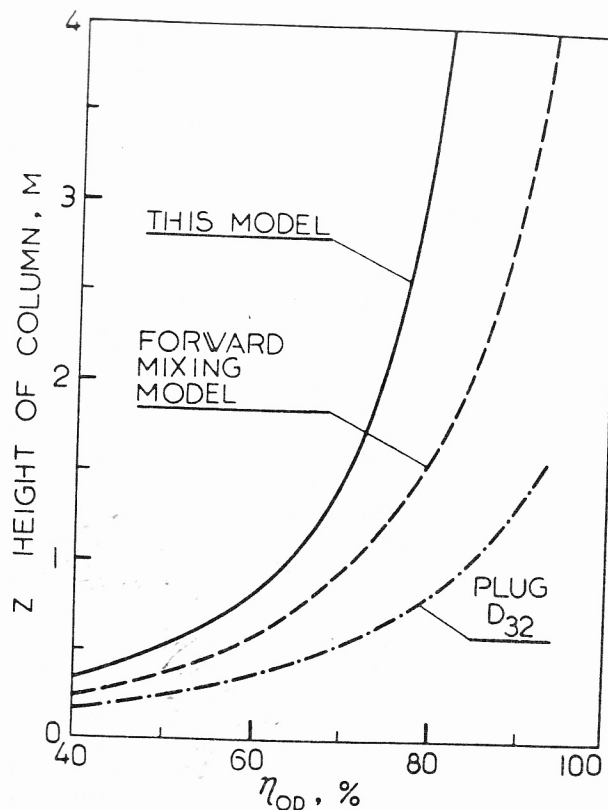


Figure 14 — Comparison of efficiencies predicted by different models.

sired extraction efficiency are also increasingly influenced by the model as efficiency increases. Hence it must be emphasized that choosing a correct model for the column performance is important.

Experimental and predicted results obtained in mass transfer runs are summarized in Table 6. The N_{ODP} values of experimental vs. predicted are also compared in Figure 15. These runs covered a large range of flowrates, agitating speed, and different mass transfer direction, either $c \rightarrow d$ or $d \rightarrow c$ direction.

The comparison of experimental, and model-predicted, number of transfer units, N_{ODP} (see Figure 15), shows that experimental values of $c \rightarrow d$ mass transfer direction were about the same as those predicted by our model when both the combined single drop models and the Calderbank and Moo-Young continuous phase mass transfer coefficient were applied. The predicted values of N_{ODP} are on the average about 6% higher than experimental ones, ranging from 82% to 126% of the experimental values. The standard deviation is 15%. In the case of $d \rightarrow c$ mass transfer direction, the predicted values of N_{ODP} are about 19% lower than the experimental ones, ranging from 69% to 94%. The standard deviation is 8.1%.

The differences between the two mass transfer directions are probably due to the effect of coalescence and redispersion of the drops. When solute transfers from continuous phase to dispersed phase, the coalescence and redispersion of the drops seldom occur, which has been confirmed by Misek (1970). Hence each drop keeps its own identity, and good results have been obtained by the model. When solute transfers in opposite direction, the coalescence and redispersion may take place, and can be explained by using interfacial phenomena i.e. Marangoni effect.

TABLE 6
Results

Exp. no.	U_c cm/s	U_d cm/s	N r.p.s.	h	d_{max} cm	a	δ	E_{OD}		N_{ODP}	
								Exp.	Pred.	Exp.	Pred.
1	0.1981	0.2617	6.67	0.0898	0.441	0.457	0.731	0.384	0.391	0.543	0.558
2	0.1309	0.2617	6.67	0.0932	0.310	0.380	0.599	0.340	0.371	0.487	0.554
3	0.2688	0.1928	9.17	0.0966	0.340	0.234	0.510	0.583	0.539	0.964	0.848
4	0.2688	0.2617	9.17	0.158	0.276	0.226	0.498	0.596	0.565	1.04	0.951
5	0.1981	0.1928	9.17	0.110	0.294	0.701	0.619	0.633	0.577	1.17	0.985
6	0.1309	0.1238	9.17	0.0523	0.344	0.426	0.715	0.573	0.508	0.971	0.795
7	0.1309	0.1928	9.17	0.114	0.230	0.395	0.633	0.527	0.521	0.910	0.892
8	0.1309	0.2617	9.17	0.137	0.299	0.477	0.576	0.447	0.440	0.742	0.722
9	0.2864	0.3130	5.00	0.101	0.517	0.319	0.526	0.321	0.374	0.417	0.513
10	0.2864	0.3130	6.67	0.112	0.557	0.352	0.742	0.347	0.392	0.464	0.547
11	0.2864	0.3130	9.17	0.128	0.425	0.311	0.453	0.425	0.469	0.616	0.714
12	0.4770	0.3130	8.33	0.145	0.383	0.146	0.437	0.456	0.533	0.651	0.825
13	0.2864	0.1450	8.33	0.0511	0.447	0.324	0.664	0.416	0.490	0.564	0.711
14	0.2864	0.5382	8.33	0.276	0.401	0.128	0.426	0.368	0.420	0.540	0.661
15	0.2688	0.1238	9.17	0.0523	0.381	0.207	0.476	0.566	0.533	0.886	0.806
16	0.2688	0.1945	9.17	0.0755	0.399	0.274	0.551	0.554	0.521	0.886	0.803
17	0.2688	0.1238	10.83	0.0613	0.330	0.418	0.861	0.687	0.632	1.26	1.07
18	0.2688	0.1928	10.83	0.0852	0.401	0.408	0.630	0.648	0.558	1.17	0.897
19	0.2688	0.2617	10.83	0.124	0.381	0.466	0.396	0.635	0.544	1.18	0.894
20	0.1981	0.1238	10.83	0.0653	0.294	0.523	0.700	0.684	0.663	1.28	1.20
21	0.1981	0.1928	10.83	0.0994	0.310	0.350	0.550	0.658	0.607	1.26	1.08
22	0.1981	0.2617	10.83	0.154	0.264	0.411	0.574	0.655	0.627	1.34	1.23
23	0.1309	0.1238	10.83	0.0784	0.312	0.720	1.16	0.748	0.667	1.66	1.29
24	0.1309	0.1928	10.83	0.0943	0.261	0.413	0.633	0.677	0.592	1.49	1.12
25	0.2829	0.1238	12.5	0.0801	0.248	0.575	0.886	0.835	0.717	1.98	1.36
26	0.2829	0.1928	12.5	0.192	0.294	0.675	1.09	0.820	0.735	2.00	1.51
27	0.2829	0.1928	12.5	0.174	0.310	0.834	0.638	0.781	0.659	1.74	1.20
28	0.2688	0.1238	12.5	0.0955	0.208	0.460	0.773	0.855	0.775	2.15	1.64
29	0.2688	0.1928	12.5	0.178	0.240	0.600	0.838	0.855	0.761	2.30	1.65
30	0.1981	0.0672	12.5	0.0568	0.209	0.569	0.762	0.862	0.786	2.14	1.65

NOTE: k_c , Calderbank and Moo-Young; $y^* = 0.05155x + 0.01320x^2$; direction of mass transfer: $c \rightarrow d$ for experiment no. 1-14 and direction of mass transfer: $d \rightarrow c$ for experiment no. 15-30.

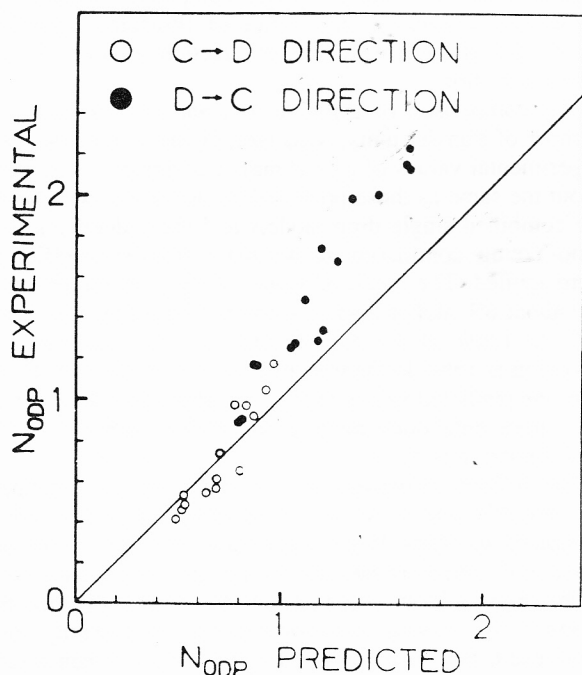


Figure 15 — Comparison of model predicted N_{ODP} and experimental N_{ODP} .

In general, the presence of solute will lower the interfacial tension ($d\sigma/dC < 0$), and it is expected that as solute transfer from drops to continuous phase, the concentration of the solute in the film between two adjacent drops is greater than the bulk concentration of the continuous phase. Hence the local interfacial tension is lowered, the drainage of the liquid film separating the drops is accelerated and the coalescence of drops is promoted. If the diameter of the coalesced drop exceeds the maximum drop size in the turbulent field, it will probably redisperse into smaller drops instantaneously. However, overall, drop size in $d \rightarrow c$ mass transfer direction is greater than that in the opposite direction.

On the contrary, when solute transfers from continuous phase to the drops, the concentration of the solute in the film between two adjacent drops is lower than the bulk concentration so that the local interfacial tension is greater and the drainage of the liquid film is retarded. Consequently, the coalescence of drops is inhibited. In this case, the drop size will be smaller than that without mass transfer or with mass transfer in $d \rightarrow c$ direction.

Coalescence and redispersion of drops not only affect the drop sizes, and therefore the characteristic velocity etc., but also affect the mass transfer behaviour of the drops in two respects. First, coalescence, in equalizing dispersed phase concentrations and thus increasing the overall concentration

difference driving force, does limit the influence of drop size distribution on extraction efficiency. Second, it perhaps is the main cause that coalescence and redispersion of drops change the concentration gradient in the drops and renew the interface of the drops so that the mass transfer coefficients in drop side will increase significantly.

Therefore, the values of experimental N_{ODP} are greater than those predicted by the model in the mass transfer direction of $d \rightarrow c$. Unfortunately, the drop interaction effect cannot be included in this mode, for the time being, since information concerning probabilities of interaction of different size drops in different conditions is not yet available.

Conclusions

1. A model including both forward mixing and axial dispersion effects has been derived and solved numerically. The large influence of drop size distribution on predicted efficiencies has been confirmed by solving the model equations.
2. Good agreement has been demonstrated between experimental overall RTDs and those predicted by the model. On the contrary, the RTDs predicted by the forward mixing model or the dispersion model have shown significant deviations.
3. The computed results have indicated that the effects of both forward mixing and dispersion of drops on extraction efficiency are significant; and the efficiency may be overestimated if only a forward mixing model is used.
4. The preliminary attempt that introduces the criterion to extend the scope of using drop mass transfer models has greatly increased the accuracy of the prediction.
5. The mass transfer data obtained in RDC are closely predicted by authors' model for $c \rightarrow d$ direction of mass transfer while about 19% greater than the predicted ones for $d \rightarrow c$ direction of solute transfer owing to the effect of coalescence and redispersion of the drops.

Acknowledgement

The authors are grateful to Professor M. H. Chen and Professor W. K. Yuan for their valuable discussion and advice.

Nomenclature

A	= absorbance
a	= asymmetrical distribution parameter
C	= concentration, g/L
C'	= constant of proportionality
D	= solute diffusivity, cm^2/s
D_R	= rotor disk diameter, cm
D_s	= stator ring opening diameter, cm
D_T	= column diameter, cm
d	= drop diameter, cm
d_{32}	= Sauter mean diameter, cm
E	= rate of energy dissipation per unit mass of fluid
$E(\tau, Z)$	= overall RTD of drops
E_D	= axial dispersion coefficient of drops, cm^2/s
E_c	= axial dispersion coefficient of continuous phase, cm^2/s
f	= transition probability density
g	= acceleration due to gravity, cm^2/s
H_T	= compartment height, cm
h	= fractional hold-up of dispersed phase
k	= individual phase mass transfer coefficient, cm/s
K_{OD}	= overall mass transfer coefficient based on dispersed phase, cm/s
L	= effective height of column, cm

m	= distribution coefficient, $y^* = m \cdot x$
N	= rotor speed, s^{-1}
N_{ODP}	= number of transfer units with plug-flow
Re	= Reynolds number ($dU_s\rho_c/\mu_c$)
T	= transmittance
t	= time, s
$U, U(d)$	= axial velocity of the drop, cm/s
U_c, U_d	= superficial velocity of continuous phase and dispersed phase respectively, cm/s
U_s	= slip velocity of the drop, cm/s
U_t	= terminal velocity of the drop, cm/s
V	= volumetric distribution of drops
v	= volumetric distribution density of drops, cm^{-1}
w	= the position of the drop at time, t
X	= concentration of continuous phase of plug-flow, g/L
x	= concentration of continuous phase, g/L
Y	= overall concentration of dispersed phase, g/L
y	= concentration of the drop, g/L
Z	= the position of the drop at time τ

Greek letters

δ	= uniformity distribution parameter
ϵ_k	= peak factor
λ	= extraction factor, $U_c/(U_d \cdot m)$
λ_n	= eigenvalue
μ	= viscosity, dyne·s/cm ²
ρ	= density, g/cm ³
τ	= time, s
σ	= interfacial tension, dyne/cm; standard deviation, see Equation (61)
Σ_k	= skewness
φ	= density of the flowrate of the drop size d , see Equation (26)
Ψ	= deviation, see Equation (38)
η	= extraction efficiency

Subscripts

c	= continuous phase
d	= dispersed phase
i	= respecting to n drop size fractions
j	= respecting to m time intervals
s	= rigid sphere model
L	= laminar circulating model
T	= turbulent circulating model

Superscripts

*	= at equilibrium; Laplace transform, see Equation (3)
---	---

References

- Calderbank, P. M. and M. B. Moo-Young, "The Continuous Phase Heat and Mass-Transfer Properties of Dispersions", *Chem. Eng. Sci.* **16**, 39-54 (1961).
- Chartres, R. H. and W. J. Korchinsky, "Modelling of Liquid-Liquid Extraction Columns: Predicting the Influence of Drop Size Distribution", *Trans. Inst. Chem. Engrs.* **53**, 247-253 (1975).
- Cruz-Pinto, J. J. C. and W. J. Korchinsky, "Experimental Confirmation of the Influence of Drop Size Distribution on Liquid-Liquid Extraction Column Performance", *Chem. Eng. Sci.* **35**, 2213-2219 (1980).
- Handlos, A. E. and T. Baron, "Mass and Heat Transfer from Drops in Liquid-Liquid Extraction", *AIChE J.* **3**, 127 (1957).
- Hinze, J. O., "Fundamentals of the Hydrodynamic Mechanism of Splitting in Dispersion Processes", *AIChE J.* **1**, 289-295 (1955).
- Jeffreys, G. V., K. K. M. Al-Aswad and C. J. Mumford, "Drop-Size and Dispersed Phase Hold-up in a Large Rotating

- Disc Contactor", *Separation Sci. Technol.* **16**, 1217-1245 (1981).
- Johnson, A. I. and A. E. Hamielec, "Mass Transfer Inside Drops", *AIChE J.* **6**, 145-149 (1960).
- Korchinsky, W. J. and J. J. C. Cruz-Pinto, "Mass Transfer Coefficients — Calculation for Rigid and Oscillating Drops in Extraction Columns", *Chem. Eng. Sci.* **34**, 551-561 (1979).
- Korchinsky, W. J. and J. J. C. Cruz-Pinto, "Modelling of Countercurrent Flow Liquid-Liquid Extraction Columns", *ISEC* **80**, 80-176 (1980).
- Kronig, R. and J. C. Brink, "On the Theory of Extraction from Falling Droplets", *Appl. Sci. Res.* **A2**, 142 (1950).
- Misek, T. and T. Marek, "Asymmetric Rotating Disc Extractor", *Brit. Chem. Eng.* **15**, 202 (1970).
- Miyauchi, T., H. Mitsutake and I. Harase, "Longitudinal Dispersion in Rotating Impeller Types of Contactors", *AIChE J.* **12**, 508 (1966).
- Newman, A. B., "The Drying of Porous Solids Diffusion Calculations", *Trans. Am. Inst. Chem. Eng.* **27**, 310 (1931).
- Olney, R. B., "Drop Characteristics in a Countercurrent Contactor", *AIChE J.* **10**, 827 (1964).
- Rod, V., "Calculating Mass Transfer with Longitudinal Mixing", *Brit. Chem. Eng.* **11**, 483-487 (1966).
- Rod, V., "Longitudinal Mixing in a Dispersed Phase in Rotating Disk Extractors", *Coll. Czech. Chem. Comm.* **33**, 2855 (1968).
- Strand, C. P., R. B. Olney and G. H. Ackerman, "Fundamental Aspects of Rotating Disk Contactor Performance", *AIChE J.* **8**, 252 (1962).
- Vermeulen, T., T. S. Moon, A. Hennico and T. Miyauchi, "Axial Dispersion in Extraction Column", *Chem. Eng. Prog.* **62**, 95-102 (1966).
- Zhang, Z. D. et al., "Study on Mass Transfer Inside Drops", *Proceeding of Inter-Collegiate Symposium on Chemical Engineering*, 63 (1963) (in Chinese).
- Zhang, S. H., X. D. Ni and Y. F. Su, "Hydrodynamics, Axial Mixing and Mass Transfer in Rotating Disk Contactors", *Can. J. Chem. Eng.* **59**, 573-583 (1981).

Manuscript received November 11, 1983; revised manuscript received August 9, 1984; accepted for publication October 15, 1984.